The effect of laser power on mechanical and physical properties of Ti-6Al-4V ELI
fabricated by selective laser melting

Miss Pajaree Termrungruanglert

จุฬาลงกรณ์มหาวิทยาลัย
CHULALONGKORN UNIVERSITY

A Thesis Submitted in Partial Fulfillment of the Requirements
for the Degree of Master of Science in Prosthodontics
Department of Prosthodontics
FACULTY OF DENTISTRY
Chulalongkorn University
Academic Year 2020
Copyright of Chulalongkorn University

อิทธิพลของกำลังเลเซอร์ต่อคุณสมบัติทางกลและทางกายภาพของโลหะเจือไทเทเนียม-อะลูมิเนียม-
วาเนเดียม อีแอลไอ ที่ขึ้นรูปด้วยวิธีการหลอมด้วยแสงเลเซอร์

น.ส.ปาจรีย์ เติมรุ่งเรืองเลิศ

Thesis Title   The effect of laser power on mechanical and physical
                      properties of Ti-6Al-4V ELI fabricated by selective laser
                      melting
By   Miss Pajaree Termrungruanglert
Field of Study   Prosthodontics
Thesis Advisor   Associate Professor VIRITPON SRIMANEEPONG, D.D.S.,
                      M.Sc., Ph.D.
Thesis Co Advisor   Professor PRASIT PAVASANT, D.D.S., Ph.D.

        Accepted by the FACULTY OF DENTISTRY, Chulalongkorn University in Partial
Fulfillment of the Requirement for the Master of Science

                ---------------------------------- Dean of the FACULTY OF
                                                  DENTISTRY
                (Associate Professor Pornchai Jansisyanont, D.D.S., M.S.,
                Ph.D.)

THESIS COMMITTEE
                ---------------------------------- Chairman
                (Assistant Professor WACHARASAK TUMRASVIN, D.D.S.,
                Ph.D.)
                ---------------------------------- Thesis Advisor
                (Associate Professor VIRITPON SRIMANEEPONG, D.D.S.,
                M.Sc., Ph.D.)
                ---------------------------------- Thesis Co-Advisor
                (Professor PRASIT PAVASANT, D.D.S., Ph.D.)
                ---------------------------------- External Examiner
                (Associate Professor Somchai Urapepon, D.D.S., Ph.D.)

iii

ปาจรีย์ เติมรุ่งเรืองเลิศ : อิทธิพลของกำลังเลเซอร์ต่อคุณสมบัติทางกลและทางกายภาพของโลหะเจือ
ไทเทเนียม-อะลูมิเนียม-วาเนเดียม อีแอลไอ ที่ขึ้นรูปด้วยวิธีการหลอมด้วยแสงเลเซอร์. (The effect
of laser power on mechanical and physical properties of Ti-6Al-4V ELI fabricated by
selective laser melting) อ.ที่ปรึกษาหลัก : รศ. ทพ. ดร.วิริทธิ์พล ศรีมณีพงศ์, อ.ที่ปรึกษาร่วม :
ศ. ทพ. ดร.ประสิทธิ์ ภวสันต์

การศึกษานี้มีวัตถุประสงค์เพื่อศึกษาความแตกต่างของคุณสมบัติทางกล และทางกายภาพของ

โลหะเจือไทเทเนียม-อะลูมิเนียม-วาเนเดียม อีแอลไอ ที่ขึ้นรูปด้วยวิธีการหลอมด้วยแสงเลเซอร์ เมื่อ
ใช้กำลังเลเซอร์ที่ต่างกัน โดยผงโลหะเจือไทเทเนียม-อะลูมิเนียม-วาเนเดียม อีแอลไอ ถูกขึ้นรูปด้วยเครื่องพิมพ์
โลหะ 3 มิติ (Trumpf/TruPrint 1000, Germany) เป็นรูปร่างดัมเบล แบ่งกลุ่มการศึกษาเป็น 3 กลุ่ม ได้แก่
กำลังเลเซอร์ 75, 100 และ 125 วัตต์ กลุ่มละ 8 ชิ้น ส่วนค่าพารามิเตอร์อื่นๆได้แก่ spot size 30 ไมโครเมตร,
ความเร็วสแกน 600 มิลลิเมตร/วินาที และความหนาแต่ละชั้น 30 ไมโครเมตร กำหนดให้คงที่ จากนั้นนำชิ้นงาน
มาทดสอบคุณสมบัติทางกล คือ การทดสอบแรงดึง และความแข็งผิวจุลภาค นำข้อมูลที่ได้มาวิเคราะห์ทางสถิติ
โดยการแปรปรวนทางเดียว (one way ANOVA) และทดสอบความแตกต่างระหว่างค่าเฉลี่ยรายคู่ (post hoc
comparisons) ด้วยการทดสอบเชิงซ้อนชนิดทูคี (Tukey's post-hoc test) ที่ระดับความเชื่อมั่นร้อยละ 95
จากนั้นนำไปวิเคราะห์โครงสร้างทางจุลภาคด้วยกล้องจุลทรรศน์แบบใช้แสง และศึกษารูปแบบของการแตกหัก
ด้วยกล้องจุลทรรศน์แบบส่องกราด พบว่าค่าเฉลี่ยแรงดึงในกลุ่มกำลังเลเซอร์ 100 วัตต์มีค่าสูงสุด โดยมีค่า
1189.67 เมกะปาสคาล นอกจากนี้ค่าเฉลี่ยความแข็งผิวจุลภาคยังมีค่าสูงสุดอีกด้วย โดยมีค่า 394.94 VHN ส่วน
กลุ่มกำลังเลเซอร์ 75 และ 125 วัตต์มีค่าเฉลี่ยแรงดึง 424.62 และ 329.88 เมกะปาสคาล ตามลำดับ และมี
ค่าเฉลี่ยความแข็งผิวจุลภาค 368.3 และ 369.62 VHN ตามลำดับ ลักษณะการแตกหัก (mode of failure)
ภายหลังการทดสอบแรงดึงในกลุ่มกำลังเลเซอร์ 75 และ100 วัตต์เป็นชนิด ductile และ brittle fracture ส่วน
ในกลุ่มกำลังเลเซอร์ 125 วัตต์ เป็นชนิด brittle fracture สรุปได้ว่าค่ากำลังเลเซอร์ที่ต่างกันส่งผลต่อคุณสมบัติ
ทางกล และทางกายภาพ โดยในกลุ่มกลุ่มกำลังเลเซอร์ 100 วัตต์มีค่าเฉลี่ยแรงดึง และความแข็งผิวจุลภาคสูงสุด
อย่างมีนัยสำคัญทางสถิติ (α=0.05). นอกจากนี้ยังพบโครงสร้างเฟส α' martensitic ในกลุ่มนี้ด้วย

สาขาวิชา   ทันตกรรมประดิษฐ์   ลายมือชื่อนิสิต ....

ปีการศึกษา   2563   ลายมือชื่อ อ.ที่ปรึกษาหลัก ....

ลายมือชื่อ อ.ที่ปรึกษาร่วม ....

Pajaree Termrungruanglert : The effect of laser power on mechanical and physical properties of Ti-6Al-4V ELI fabricated by selective laser melting . Advisor: Assoc. Prof. VIRITPON SRIMANEEPONG, D.D.S., M.Sc., Ph.D. Co-advisor: Prof. PRASIT PAVASANT, D.D.S., Ph.D.

This study aimed to examine the differences in mechanical and physical properties of Ti-6Al-4V *extra low interstitial* (ELI) fabricated by selective laser melting (SLM) between different laser power. The Ti-6Al-4V ELI alloy samples were printed in dumbbell shape by SLM machine (Trumpf/TruPrint 1000, Germany) with 3 laser powers (75, 100 and 125 W), 8 samples for each group. And the other parameters (spot size 30 μm, scanning speed 600 mm/s, layer thickness 30 μm) were kept constantly. All samples were performed under tensile test with universal testing machine. Moreover, The microhardness test was performed. All data were statistically analyzed with one way ANOVA and Tukey's post-hoc tests (α=0.05). The microstructure was analyzed by optical microscope and mode of failure was observed by SEM. It was found that the group laser power 100 W was the highest mean tensile strength (1189 .67 MPa) and highest mean microhardness (394.94 VHN). The tensile strength in group laser power 75 and 125 W were 424.62 and 329.88 MPa, respectively. And microhardness value in group laser power 75 and 125 W were 368.3 and 369.62 VHN, respectively. Mode of failure after tensile testing in group of laser power 75 and 100 W showed in both ductile and brittle fracture. And the group of laser power 125 W was predominantly brittle fracture. In conclusion the difference in laser power effected the mechanical and physical properties. The laser power 100 W showed the highest mean tensile strength and microhardness significantly compared to the other 2 groups (α=0.05). And this group was found the α' martensitic phase microstructure.

Field of Study: Prosthodontics   Student's Signature ....

Academic Year: 2020   Advisor's Signature ....

                                                Co-advisor's Signature ....

ACKNOWLEDGEMENTS

TABLE OF CONTENTS

LIST OF TABLES

LIST OF FIGURES

CHAPTER I INTRODUCTION

Background and rationale

Titanium is being used increasingly for a variety of application. Examples include aircraft, aero-engines, components in chemical processing equipment and also in biomedical fields(1). There are the most widely use of titanium as an implant in biomedical fields because it is dominant in many properties such as good biocompatibility, high corrosive resistance, high specific strength, nonmagnetic property and low specific gravity. The orthopedist uses an implant in many ways including total hip replacement (THR), total knee arthroplasty (TKA) and it is used as a dental implant in dentistry (2).

Titanium grade 23 or Ti-6Al-4V ELI is titanium alloy. Ti-6Al-4V ELI is basically a titanium grade 5 but the amount of oxygen(O), Iron(Fe), nitrogen(N) are less for low interstitial alloy. This can improve ductility and fracture toughness with some reduction in strength. To meet the requirement of medical implant, the mechanical properties must follow ASTM F136-13 that require yield strength more than 795 MPa, ultimate tensile strength above 860 MPa and at least 10 percent of elongation. There are many methods to fabricate the titanium implant such as casting, cold-working or cast bar stock by Computer Numerical Control (CNC). These methods are the subtractive manufacturing. The disadvantages of the subtractive manufacturing are waste of material, not accuracy, and it is not cost effective for some processing.

Recently, Additive manufacturing (AM) has been developed for fabrication of the titanium. AM is also commonly known as 3D printing. It is a process of joining material to make objects from 3D model data, usually layer by layer. Selective laser melting (SLM) is one of the 3D printing technology. It starts with creating a 3D model of a product using computer aided design (CAD) software followed by sliced in thin layers. The 3D file is usually a STereoLithography(.stl) file format (3-5). After that all the layers are sent to a SLM device in order to realize the final product on the basis of layer by layer. The benefits of selective laser melting(SLM) over the traditional production methods are reducing material consumption, fabricates complex implant. Moreovers, It could create intricate details of the design or the complexity that is

hard to successed with traditional productions.

In the manufacturing process of SLM, Firstly, a building platform is moved down. Then the metal powder is deposited and melted forming a liquid pool by the interaction of a laser beam. The molten pool will solidify and cool down quickly. Then the building platform moves lowered again. The unmelt powders are deposited. After fabrication of the first layer, the manufacturing process is repeated for the layers until all of the layers of the component generated is complete (6).

Generally, The primary objective in SLM process is acquiring the whole object with full density and free of defects (1). To achieve this goal, there are many factors or parameters involving laser power(W), scan speed(mms^{-1}), layer thickness(mm) and scan spacing or hatch space(mm)(7). All of these factors affect the laser energy density (J) which could affect the densification and the quality of work piece (1).

There have many researches that study the effects of the parameters. However, the relationship of the laser power to the mechanical property of Ti-6Al-4V ELI is not completely understood, and more systematic research work is necessary in order to attain a better understanding of these features. In this research, the samples are fabricated at different laser powers. There are many studies investigate the result when varying the factor. But most of them usually varying multi factors and using the statistic for calculating. So this study aims to vary only the laser power by fixing others parameters including scan speed, layer thickness and scan spacing.

Research question

      1. Are there any differences in mechanical properties of SLM Ti-6Al-4V ELI between varying laser power?

      2. Are there any differences in physical properties of SLM Ti-6Al-4V ELI between varying laser power?

Research objective

      1. To examine the differences in mechanical properties of SLM Ti-6Al-4V ELI between different laser power.

      2. To examine the differences in physical properties of SLM Ti-6Al-4V ELI between different laser power.

Research hypotheses

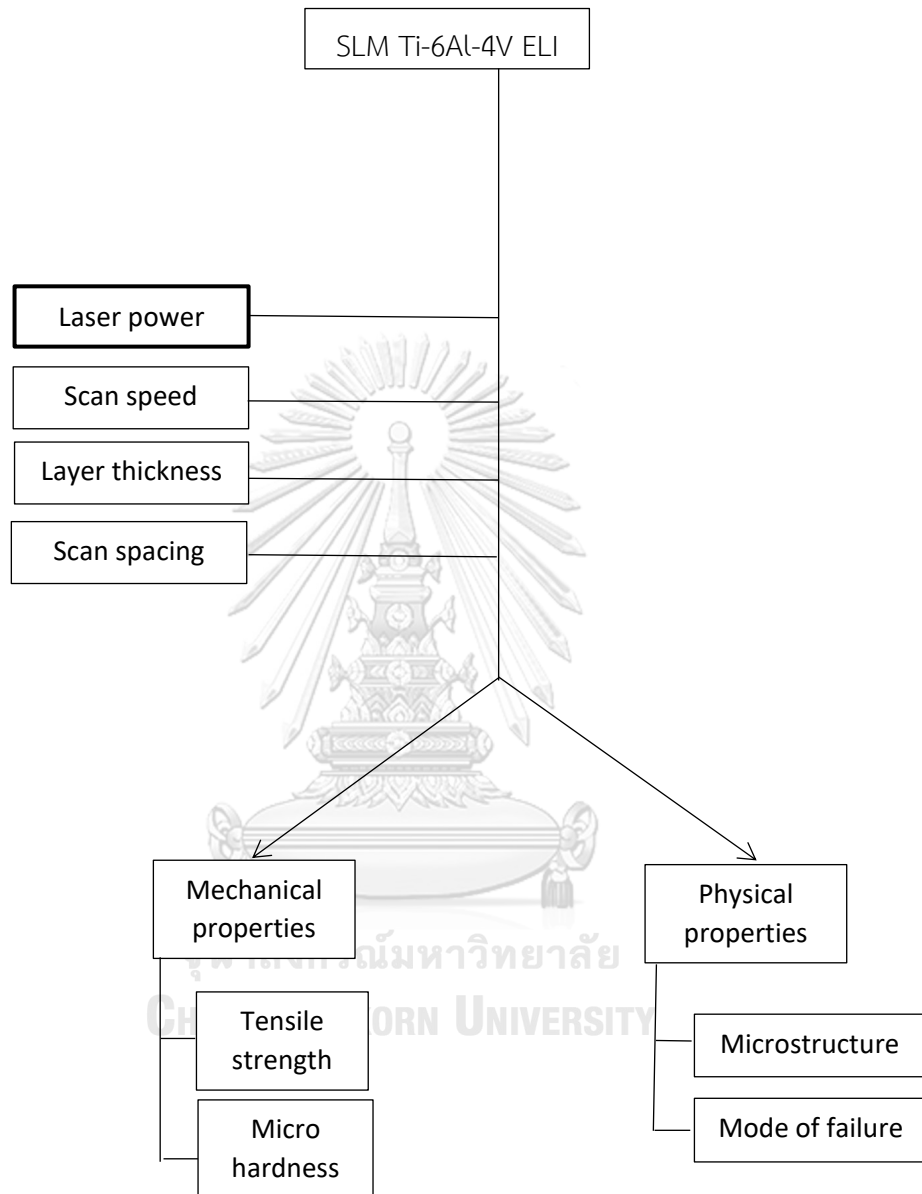   I. H0 : There is no difference of mechanical properties among Ti-6Al-4V ELI by varying laser power.

      H1 : There is a difference of mechanical properties among Ti-6Al-4V ELI by varying laser power.

      II. H0 : There is no difference of microstructure among Ti-6Al-4V ELI by varying laser power.

      H1 : There is a difference of microstructure among Ti-6Al-4V ELI by varying laser power.

Conceptual framework

```
                              ┌─────────────────────┐
                              │   SLM Ti-6Al-4V ELI │
                              └─────────────────────┘
                                         │
   ┌──────────────────┐                  │
   │   Laser power     │──────────────────┤
   └──────────────────┘                  │
   ┌──────────────────┐                  │
   │   Scan speed      │──────────────────┤
   └──────────────────┘                  │
   ┌──────────────────┐                  │
   │  Layer thickness  │──────────────────┤
   └──────────────────┘                  │
   ┌──────────────────┐                  │
   │   Scan spacing    │──────────────────┤
   └──────────────────┘                  │
                              ┌───────────┴───────────┐
                              ▼                       ▼
                    ┌──────────────────┐    ┌──────────────────┐
                    │   Mechanical     │    │    Physical      │
                    │   properties     │    │   properties     │
                    └──────────────────┘    └──────────────────┘
                         │                       │
                    ┌──────────────────┐    ┌──────────────────┐
                    │    Tensile       │    │  Microstructure  │
                    │    strength      │    └──────────────────┘
                    └──────────────────┘    ┌──────────────────┐
                    ┌──────────────────┐    │  Mode of failure │
                    │      Micro       │    └──────────────────┘
                    │    hardness      │
                    └──────────────────┘
```

Proposed benefits

The outcomes of this study may provide understanding the role of laser power on the properties of SLM Ti-6Al-4V ELI.

CHAPTER II LITERATURE REVIEW

Additive manufacturing

Additive manufacturing (AM), also commonly known as 3D printing. American Society for Testing and Materials (ASTM) has defined this technology as "a process of joining materials to make objects from 3D model data, usually layer by layer, as opposed to subtractive manufacturing methodologies". In accordance to ISO 17296-2:2015 AM technique can be classified into 7 categories. There are photopolymerisation, material jetting, binder jetting, sheet lamination, material extrusion, powder bed fusion (PBF), and directed energy deposition (DED) (Fig 1). The most widespread AM technique for metals is powder bed fusion (PBF) process(2, 8, 9).   Powder bed fusion (PBF) is a process that use the energy of the laser (usually an ytterbium laser) to fuse the selective powder for creating a desired shape. It is controlled by the galvanometer, and the movement of the beam is controlled by the F-theta lens(10). The process using through computer aided design(CAD) data(8, 11). According to ASTM F2792-12a, both selective laser melting(SLM) and electron beam melting (EBM) are classified as powder bed fusion(10). Selective laser melting(SLM) is a process using the laser to melt the metallic powder to deposite layer by layer in an protective atmosphere (inert-gas-filled chamber). An inert atmosphere is usually argon to ovoid oxidation during the melting of the powder(12-14).   Firstly, it starts with creating a 3D model of a product using computer aided design (CAD) software followed by sliced in thin layers. Usually, the 3D file is a STereoLithography(.stl) file format(3-5).   Stl files of the layers are sent to a SLM device in order to realize the final product on the basis of layer by layer.

In the manufacturing process, a building platform is moved down firstly. Then the metal powder is deposited and melted forming a liquid pool by the interaction of a laser beam. The molten pool will solidify and cool down quickly or called the melt pool formation. Then the building platform moves lowered again. Then, the unmelt powders are deposited. After fabrication of the first layer, the manufacturing process is repeated for the layers until all of the layers of the component generated is complete(6). Once the SLM process is complete, the supporting is removed from

the built platform.

There are many advantages of SLM including fabrication of complex shapes, decreasing material waste and reducing the production cost. SLM has enabled clinicians to provide a customized implant(15).
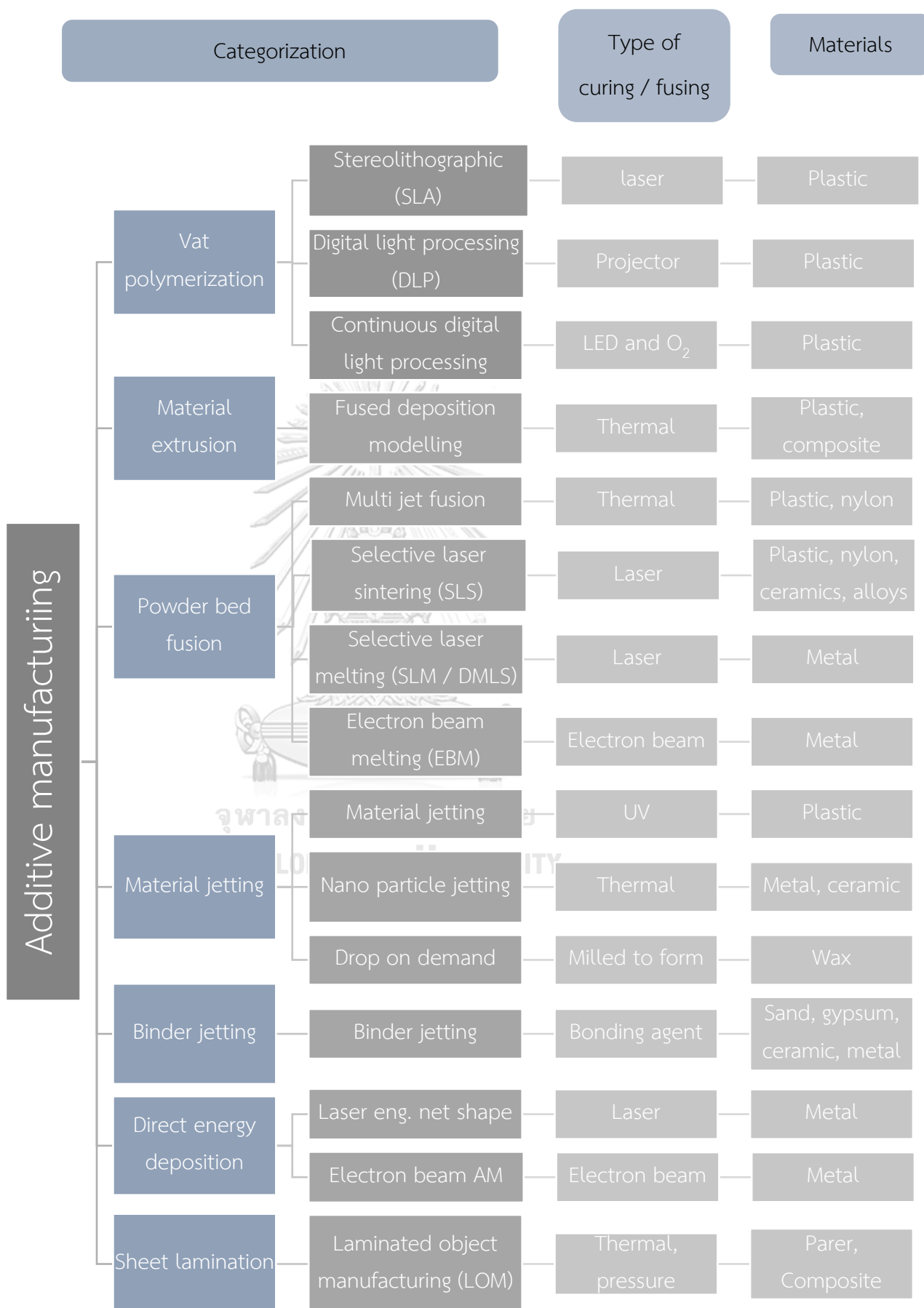
Categorization			Type of curing / fusing	Materials
Vat polymerization		Stereolithographic (SLA)	laser	Plastic
		Digital light processing (DLP)	Projector	Plastic
		Continuous digital light processing	LED and O_2	Plastic
Material extrusion		Fused deposition modelling	Thermal	Plastic, composite
Powder bed fusion		Multi jet fusion	Thermal	Plastic, nylon
		Selective laser sintering (SLS)	Laser	Plastic, nylon, ceramics, alloys
		Selective laser melting (SLM / DMLS)	Laser	Metal
		Electron beam melting (EBM)	Electron beam	Metal
Material jetting		Material jetting	UV	Plastic
		Nano particle jetting	Thermal	Metal, ceramic
		Drop on demand	Milled to form	Wax
Binder jetting		Binder jetting	Bonding agent	Sand, gypsum, ceramic, metal
Direct energy deposition		Laser eng. net shape	Laser	Metal
		Electron beam AM	Electron beam	Metal
Sheet lamination		Laminated object manufacturing (LOM)	Thermal, pressure	Parer, Composite

Additive manufacturing

Figure 1 categorization of additive manufacturing (3D printing), together with the types of curing/fusing and materials

In SLM, many parameters influence the density of the work piece(1). The main parameters are laser power, scan speed, layer thickness and scan spacing or hatch space (7). The schematic of selective laser melting (SLM) parameters is shown in fig.2. All of the factors affect the laser energy density (J) that effects the density and the quality of work piece. So it is neccessary to control these parameters for achieving the quality of the work piece. The full density and free of defects is a primary objective for this technology (1).
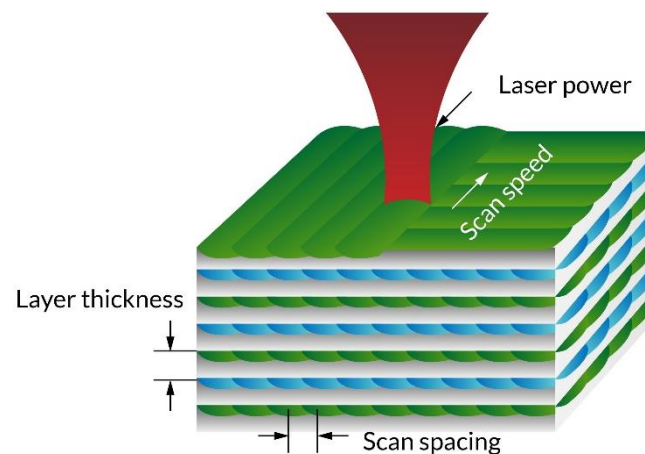
Figure 2 Schematic of selective laser melting (SLM) parameters.

During the SLM processing, power of laser beam interacts to the powder bed with the constant scan speed. Layer thickness is an each layer of powder. Moreover, scan spacing or hatch space defined the overlap of adjacent solidified metal therefore, it significantly affects the porosities and surface roughness (16).

The correlation of these factors are following to the equation (12, 17).

$$\text{Laser energy density} = \frac{laser\ power}{scan\ speed \times layer\ thickness \times scan\ spacing}$$

From this equation, to gain the laser energy density, it can be done by increasing laser power or decreasing scan speed or layer thickness or scan spacing. However, we need the minimum critical laser energy density to manufacture the maximum density. For example, the minimum critical laser energy density of Ti-6Al-4V is 120 J (12).

Effect of processing parameters

The processing parameter (e.g., laser power, scanning speed, hatch spacing and layer thickness) can significantly affect the microstructure formation during the solidification, and finally determine the resultant properties of the SLM metal (18). A mixture of alpha phase, beta phase and acicular martensitic phase has been observed in the microstructure SLM Ti-6Al-4V. The presence of acicular α' martensites in the SLM Ti-6Al-4V leads to the significant improvement in tensile strength from 900 to 1450 MPa but considerably reduced ductility (6).

The first parameter is laser power. According to the study by Mahmoud Elsayed and Hahn Choo et al. in 2019, they found that higher laser power, leads to higher energy density to generate large recoil pressures, improve the wettability of the melt pool, transfers the depths of heat penetration and eliminate the differences in surface tension(19, 20). Consequently, the surface of SLM samples have less porosity which resulting that, the roughness of both top and side surface of the SLM parts could be reduced significantly. Moreover, the mechanical properties would be improved by increasing the Young's modulus (20, 21). The second parameter is scanning speed. The scanning speed effect the melting pool. The low scanning speed cause the normal melting pools while the high scanning speed creates the irregular melting pool with multiple boundaries in SEM images (21). Using very high scanning speeds may decrease the bonding between the deposited layers and consequently reduce the mechanical properties (22). There is the research in Sc- and Zr- modified Al-Mg alloys (commercially known as Scalmalloy) found that if the scan speed increasing, the fine grain region is decreased and it is a solid solution. While laser scan speed is low, it will form the precipitation (23).

"Linear energy density" (LED) is an integrated parameter to investigate the combined effect of laser power and scan speed. The LED correlation is following to the the equation.

$$\text{Linear energy density} = \frac{laser\ power}{scan\ speed}$$

It is used to estimate the laser energy input to the powder layer being melted (24). Chandrakanth Kusuma et al. investigated LED of commercially pure titanium (CP-Ti) by studying in a single bead on the melt pool formation by varying the laser power and scan speed while the laser beam diameter and layer thickness were kept constant. They used optical microscope to study the melt pool shape. They found that high laser power and slow scan speed or high energy density lead to wider melt pools, whereas low laser power and high scan speed or low energy density results in narrow melt pools (19). Layer thickness is important parameter because the metal powder of each layer can be totally melted that subsequent contributes to good connecting between layer. While powder layer is thicker that will lead to increase nodulizing tendency and unmelt layer resulting in low density (25). The last parameter is scan spacing or hatching space. Density fluctuates in a narrow range with the increasing hatching space. Small hatching space increases the overlapping area of adjacent scanning lines, which generates the overlying of laser beams energy. As a result, the uniform distribution of energy will make the powder between scanning lines melt completely, and the depth of melting lines tends to be even. The subsequent melting liquid grows on the solidified scanning lines and substrate (i.e. solidified layer). In this way, each scanning line proceeds stably from melt to solid. However, the over-concentrated laser energy created by an extremely small scanning gap will bring overburning which influences density of samples (25).

After produced the work piece, the as-built material can be utilized without further processing or treatment (26). However, heat treatment can improve the mechanical property such as tensile properties and hardness (13, 27, 28). It can reduce the residual stress and change the microstructure by changing the original martensite alpha phase into a lamellar mixture of alpha and beta phases(8, 18). Recently the porous structure has been developed instead of solid structure to

reduce the Young's modulus. Because the young modulus of Ti-6Al-4V is 94 GPa while the bone in human body ranges from 10 to 30 GPa (17). The difference of this young modulus mismatch is often called "stress shielding" that can affect implant failure (3). So the titanium using for orthopaedic surgery having an average pore size ranging from 400 to 600 μm with the volume porosity of 75-85% can reduce the Young's modulus of material (10, 20, 29). Moreovers, the porous scaffolds can allow the growth of osteoblast for osseointegration (16). SLM has enabled clinicians to provide a customized implants which have a complex shape. Moreover, SLM can manufacture workpieces with low-cost production and minimize material waste compared to the traditional production methods such as wrought or cast bar stock by Computer Numerical Control (CNC), CAD-driven machining or powder metallurgy (PM) production methodologies (30). Murr et al. and Shunmugavel et al. found that additive manufactured Ti-6Al-4V offers higher strengths and yield strengths compared to the wrought components. Because the microstructure of SLM titanium alloys consists of columnar prior beta grains transform into a α' fully martensitic while the microstructure of wrought Ti-6Al-4V is spheroidite structure containing α phase(Hexagonal close packed, HCP structure) and β-phase (Body center cubic, BCC structure) (26).

SLM technology is applicable in 29 common metals and alloy powder material (shown in table 1)(12, 31).

	Material
Aluminium alloys	AlSi10Mg, AlSi7Mg, AlSi12
Cobalt based alloys	ASTM F75, CoCrWC
Tool steels	AISI 420, Marage 300, H13, AISI D2, AISI A2, AISI S7
Nickel based alloys	Inconel 718, Inconel 625, Inconel 713, Inconel 738, Hastelloy X
Stainless steels	SS 304, SS 316 L, SS 410, SS 440, 15-5 PH, 17-4 PH
Titanium alloys	Titanium grade 2, Ti-6Al-4V ELI, TiAl6Nb7

Precious metal alloys	Jewellery gold, Silver
Copper alloys	CC 480K

Table 1 Available metal and alloy powder material in SLM

Nowadays, AM technology has a role in medical and dentistry fields. In dentistry field, SLM could produce cobalt-chrome RPD framework, crown, bridges and dental implants(8, 32). This technology can save times when comparing with traditional method that involves waxing, investing, casting and finishing (16). In medical field, SLM can produce the implant on the diagnostic investigation such as computer tomography (CT), magnetic resonance imaging (MRI) and scanning model (33). All of the data can transfer to STL format (31). For application in orthopaedic fields, the surgeon creates a component organ such as knee, hip and acetabular cups for suitable each patients. Moreovers, European Conformity (CE) and the United States Food and Drugs Administration (FDA) have certified the SLM implant since 2007 and 2010 respectively (10).

In biological field, 3D printing can be used to create a customized bone scaffold for tissue regeneration by selective laser sintering and inkjet-based printing. The bone scaffold materials are calcium phosphate ceramic, hydroxyapatite, calcium phosphate ceramics, hydroxyapatite, calcium phosphate cements, monetite, or brushite bone. The porosity in the scaffold implant is important to encourage the bone ingrowth. The ideal porosity and pore size of the 3D printed scaffold have been reported as 30-70% and 500-1000 μm respectively (34).

In pharmacokinetics, there are drug delivery devices which are fabricated by inkjet-based 3D printing. The drug delivery devices are the binder (a solution that is able to solubilize the chosen powder) that is porous containing the drug. The benefit of this technique when compared to the traditional systemic treatment are to facilitate controlled the drug releasing and can direct to the target tissue.

Titanium

Titanium and its alloys are most widely use as a metallic biomaterial (10). Due to biocompatibility, high corrosive resistance, high specific strength, nonmagnetic property and low specific gravity so it is popular for medical and dental application (3, 6). Especially in Orthopedic and cardiovascular application. For orthopedic, they use titanium as plates and screw to stabilize the bone. Moreover, it can be used as an artificial bone for the organ replacement such as total hip replacement (THR), total knee arthroplasty (TKA), dynamic compression plate (DCP) and lumbar fusion and fixation (10, 35, 36).

ASTM grades Titanium into 4 grades (grade 1 to 4) as unalloyed titanium while grade 5 is titanium alloyed (Ti-6Al-4V). Titanium alloys usually has higher corrosion resistance compared to commercially pure titanium (37).

Titanium grade 5, also known as Ti-6Al-4V (Ti64). It is comprised of 90% titanium, 6% aluminium and 4% vanadium. Also, It is consist of an $\alpha + \beta$ titanium alloy or biphasic microstructure (3, 38). The alpha phase is stabilized by alumina. The alpha phase helps in corrosion resistance but it is low in tensile strength. The beta phase is stabilized by vanadium. The beta phase helps in ductility and resistance in plastic deformation (3).

Titanium grade 23 or Ti-6Al-4V ELI is basically a grade5 titanium but the amount of oxygen(O), Iron(Fe), nitrogen(N) are less for low interstitial alloy (shown in table 2). It improves ductility and fracture toughness with some reduction in strength.

Grade	Al	V	O	Fe	C	H	N	Other impurities total
5(39)	5.5-6.75	3.5-4.5	≤0.2	≤0.3	≤0.08	≤0.015	≤0.05	≤0.4
23(ELI)(39)	5.5-6.5	3.5-4.5	≤0.13	≤0.25	≤0.08	≤0.0125	≤0.03	≤0.3

Table 2 Composition of Ti-6Al-4V in grade 5 and grade 23.

The titanium grade 5 and 23 as biomaterial implant must be designed following the standard of ASTM or ISO (shown in table 3).

Type	ASTM standard	ISO standard	ISO standard (Method of testing)
Ti-6Al-4V	ASTM F 1472-14	ISO 5832-3	ISO 6892
Ti-6Al-4V ELI	ASTM F 136-13	ISO 5832-3	ISO 6892

Table 3 ASTM and ISO standard of titanium grade 5, 23.

The previous study showed that Ti grade 5 and 23 have yield strength more than 780 MPa, ultimate tensile strength above 860 MPa and 8-10 percent of elongation. These mechanical properties are indicated as medical applicable.

Titanium can manufactured by casting, wrought, and additive manufacturing. Although almost 70% of titanium product is manufactured by wrought (30). But nowadays AM is gained wide spread because the advantage over traditional methods for example reducing material consumption by 40 percent and fabricates complex application (3, 8, 31).

In 2017, Manikandakumar et al. found that SLM Ti-6Al-4V offers good mechanical property when compared to wrought Ti-6Al-4V (40). They found that wrought Ti-6Al-4V has yield strength in 948 MPa, ultimate tensile strength in 994 MPa, elongation in 21 percent, hardness in 306. While SLM Ti-6Al-4V has yield strength in 964 MPa, ultimate tensile strength in 1041 MPa, elongation in 7 percent, hardness in 356 (40).

Besides SLM, titanium can fabricated by electron beam melting (EBM). EBM is similar manufacturing process to SLM but it uses electron beam energy to melt the metal powder. Moreover, the SLM operates in argon gas while EBM operates under vacuum to prevent energy dissipation before delivering the beam to the work piece (1). The SLM Ti-6Al-4V has a better mechanical properties when compared to EBMed Ti-6Al-4V (shown in table 4)(10). The microstructure after cooling rate is significant to determine the mechanical properties. In SLM, the temperature of the build chamber

is 30-60˚C causing high cooling rate, resulted in a harder martensitic phase. While the temperature of EBM is 650-750 ˚c causing low cooling rate that does not allow the transformation of α to martensitic phase(10).

	SLM	EBM	Casting
Ultimate tensile strength (MPa)	1250-1267	830-1150	934-1173
Yield strength (MPa)	1110-1125	915-1200	862-999
Elongation (%)	6-7	13-25	6-7
Microhardness (HV)	476-613	358-387	294-360

Table 4 Mechanical properties of Ti-6Al-4V fabricated by SLM, EBM and casting (10).

Chapter III Material and methods

Equipments

1. Selective Laser Melting machine (Trumpf/TruPrint 1000, Germany).

2. Ti-6Al-4V ELI alloy powder (Ti grade 23) (AP&C, USA)

3. Universal testing machine (SHIMADZU AGS-X 100kN model, Japan)

4. Microhardness test (FM-810e, FUTURE-TECH, Japan)

5. Optical microscope (BX51M, Olympus, Japan)

6. Scanning electron microscope (FEI Quanta 250, USA)

7. Wheel cut machine

8. 400, 600, 800, 1000, 2000 Silicon carbide grinding paper

9. Polishing machine (Minitech 233, Presi, Le Locle, Switzerland)

10. Vernier caliper (Mitutoyo, Japan)

Methodology

1. Sample preparation and SLM process

Ti-6Al-4V ELI alloy (Ti grade 23) (AP&C, USA) chemical compositions of the meatal powder were presented in table 5. The powder had a spherical shape. The sample was fabricated by varying the laser powers into 3 groups (75, 100 and 125 W), 8 samples for each group. The other manufacturing parameters were defined by an internal algorithm (spot size 30 μm, scanning speed 600 mm/s, layer thickness 30 μm) of the 3D metal printer (Trumpf/TruPrint 1000, Germany).

Al	V	Fe	O	C	N	H	Ti
5.5-6.5	3.5-4.5	<0.25	<0.13	<0.08	<0.05	<0.012	Balance

Table 5 Chemical composition of Ti-6Al-4V ELI metal powder

The powder of Ti-6Al-4V ELI was printed in dumbbell shape in diameter of 9 mm.(D) and gauge length in 26 mm.(G) accordanced with ASTM E 8M-04 (41) and followed the size of grip in universal testing machine. No post-treatment will be applied to the sample. All printed samples were measured for density by electronic densitometer (AlfaMirage, MD-300S, Australia).
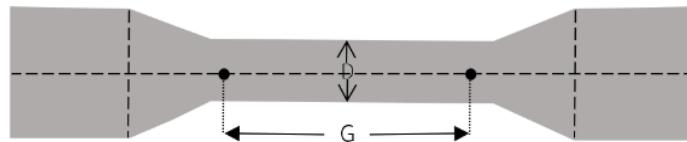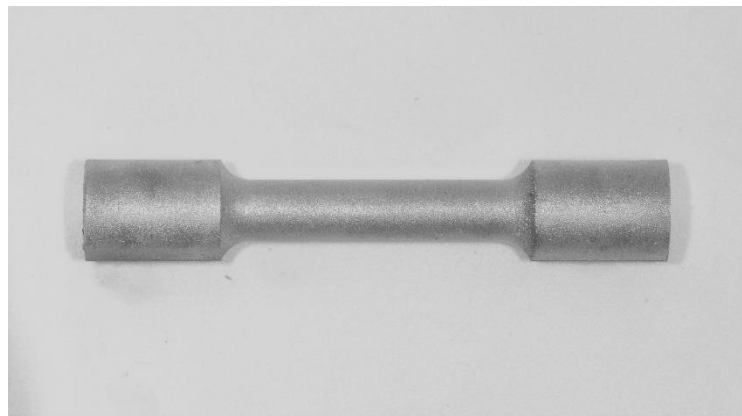
Figure 3 The geometry and dimension of the sample

Figure 4 Sample

2. Tensile test

The tensile tests were performed using the universal testing machine (SHIMADZU 100kN, Japan) at room temperature which was equipped with a 1.0 kN load cell enabling the force measurement with a precision of 0.1 N. A tensile load was applied at a crosshead speed of 0.3 mm/min. The data were collected and recorded automatically by the computer-based control and data acquisition system during the tensile process. The test was performed until the sample was broken.

Figure 5 Universal testing machine (SHIMADZU AGS-X 100kN model, Japan)

Figure 6 The grip of universal testing machine held the sample.

3. Physical property

3.1 Mode of failure

After fractured from tensile test, the specimen were visually analyzed under scanning electron microscope (SEM) (FEI Quanta 250, USA) at x100 and x300 magnification to analyze modes of failure. Failure modes were classified into three types. There were ductile fracture, brittle fracture and combined fracture with ductile and brittle fracture.

Figure 7 Fractured sample after tensile testing

3.2 Observation microstructure

Then the samples from all groups were randomly prepared for microstructure analysis. And the samples were embedded in bakelite moulding in diameter 1 inch. The mounted specimens were polished using a polishing machine (Nano 2000, Pace technologies, USA) up to 2000 SiC paper then etched with Kroll's reagent (100 mL H_2O, 5 mL HNO_3 and 2.5 mL HF) for 20 seconds following ASTM E 407 and rinsed with deionized water for 20 seconds. Microstructure of the specimens were observed by optical microscope (BX51M, Olympus, Japan) at x500 magnification.

Figure 8 Prepared sample after polishing in bakelite moulding

4. Microhardness test

Microhardness of the sample were measured by microhardness tester (FM-810e, FUTURE-TECH, Japan). The samples were test using a Vicker hardness tester with a load of 5 N and loading time 15 seconds. The first indentor started below the junction of the sample and the bakelite moulding. The values reported in this study were each average values of 30 individual microhardness measurements in accordance with ASTM E 384.

5. Statistical analysis

Shapiro-Wilk and Levene's test were performed for checking normality and homogeneity of variances, respectively by SPSS (statistical analysis software version 22.0, Chicago, IL, USA). One way ANOVA and Tukey's post-hoc analysis was used to analyze tensile strength and microhardness. Significance level was set at α = 0.05.

Chapter IV Result

Mechanical properties

1. Ultimate tensile test

It was found that the group of laser power 100 W had the highest tensile testing. One way ANOVA and Tukey's post-hoc analysis presented that the tensile strength in group of laser power 75 and 100 W was significantly decreased to 424.63 and 329.88 MPa respectively ($\alpha=0.05$).

Laser power (Watt)	N	Mean and SD (MPa)
75	8	424.63 ± 54.7^A
100	8	1189.67 ± 19.05^B
125	8	329.88 ± 55.35^C

Table 6 Ultimate tensile strength

Different capital superscript letters indicate that tensile strength values were significantly different at $p<0.05$.
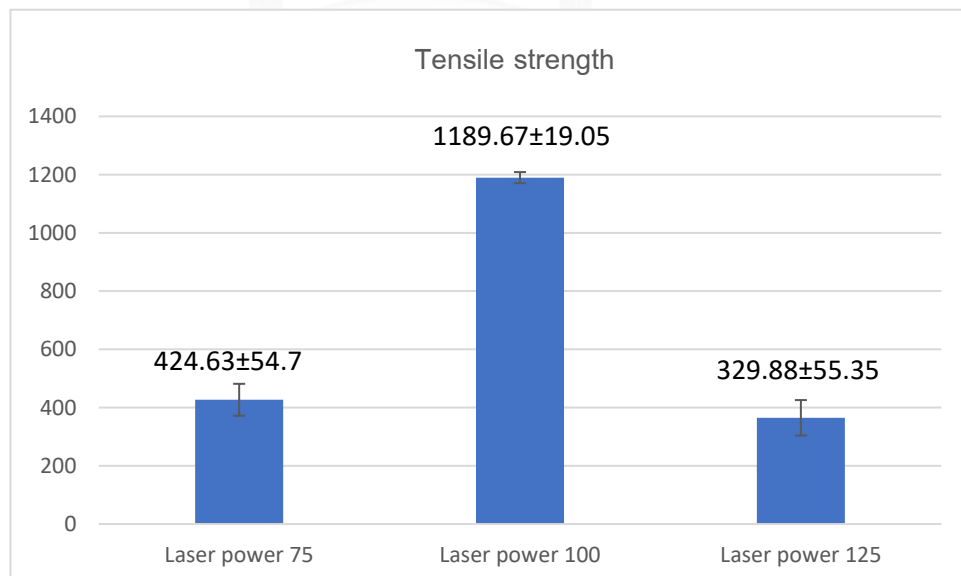
Figure 9 Tensile strength (MPa). Value presented by means ± SD

2. Microhardness test

The microhardness value was corresponding to the value of the tensile strength. The group of laser power 100 was significantly highest microhardness. And in the group of laser power 75 and 125 were 368.3 and 369.62 VHN but were not significantly different between this two groups (α=0.05).

Laser power (Watt)	N	Mean and SD (VHN)
75	30	368.3 ± 13.69^A
100	30	394.94 ± 15.16^B
125	30	369.62 ± 28.31^A

Table 7 Microhardness

Different capital superscript letters indicate that tensile strength values were significantly different at p<0.05
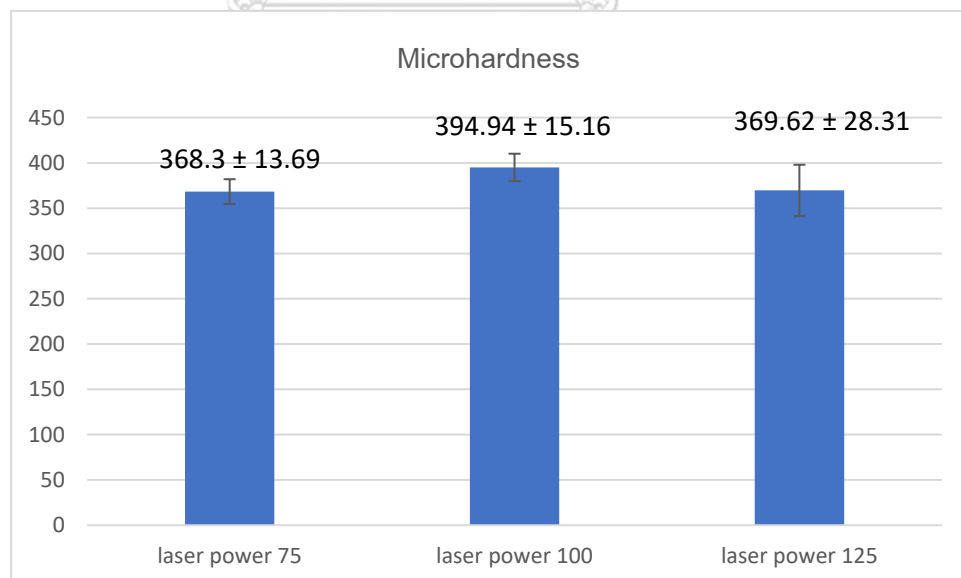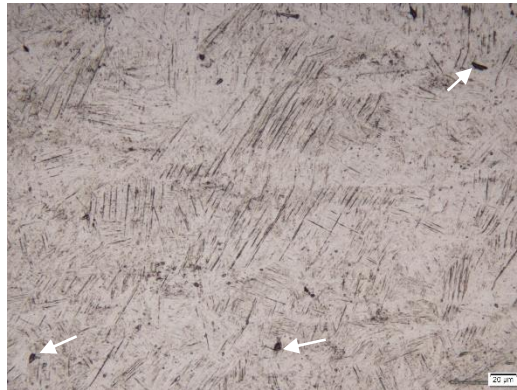

Figure 10 Microhardness (VHN). Value presented by means ± SD
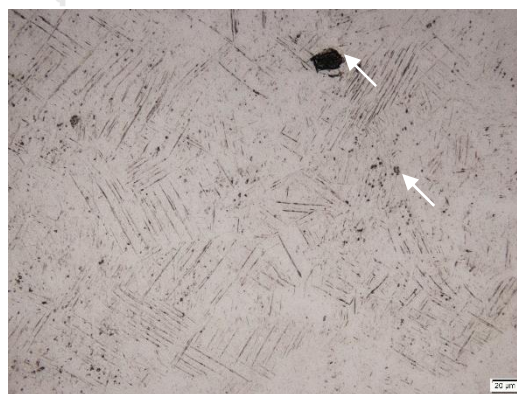
Physical properties

    1. Microstructure

(a)

(b)

(c)

Figure 11 Light optical microscope images of 3 different SLM Ti-6Al-4V ELI groups at x500 magnification (a)75W, (b)100 W and (c)125 W. The white arrows indicate the porosity. The dark arrows indicate the presence of α′ martensitic phase.

From light optical microscope at x500 magnification, we could found the α′ martensitic phase in every groups but it was dominantly presented in the group laser power 75 W (Figure 11a) and 100 W (Figure 11b). The defect or the porosity mostly found in the group laser power 75 W (Figure 11b) and 125 W (Figure 11c).

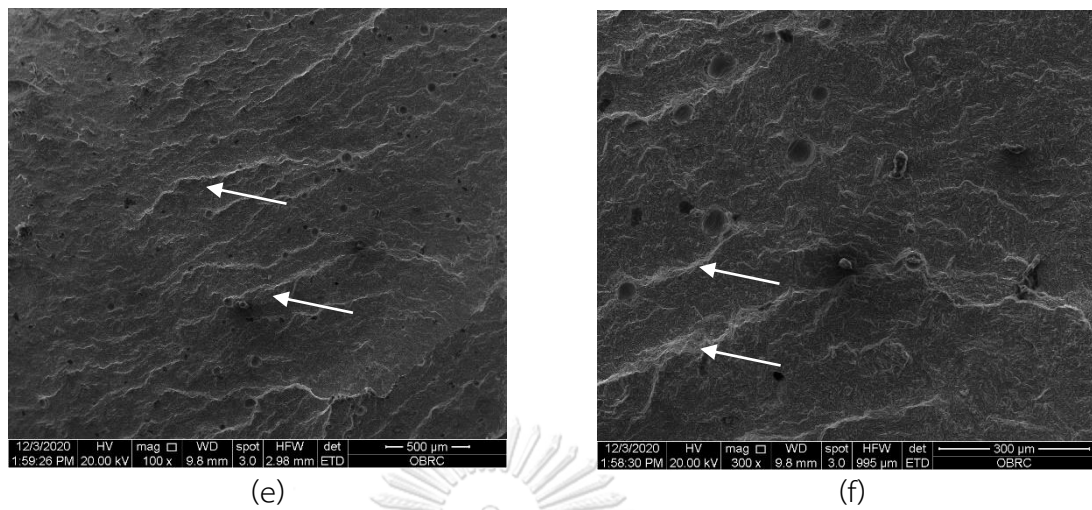2. Mode of failure

(a) (b) (c) (d)
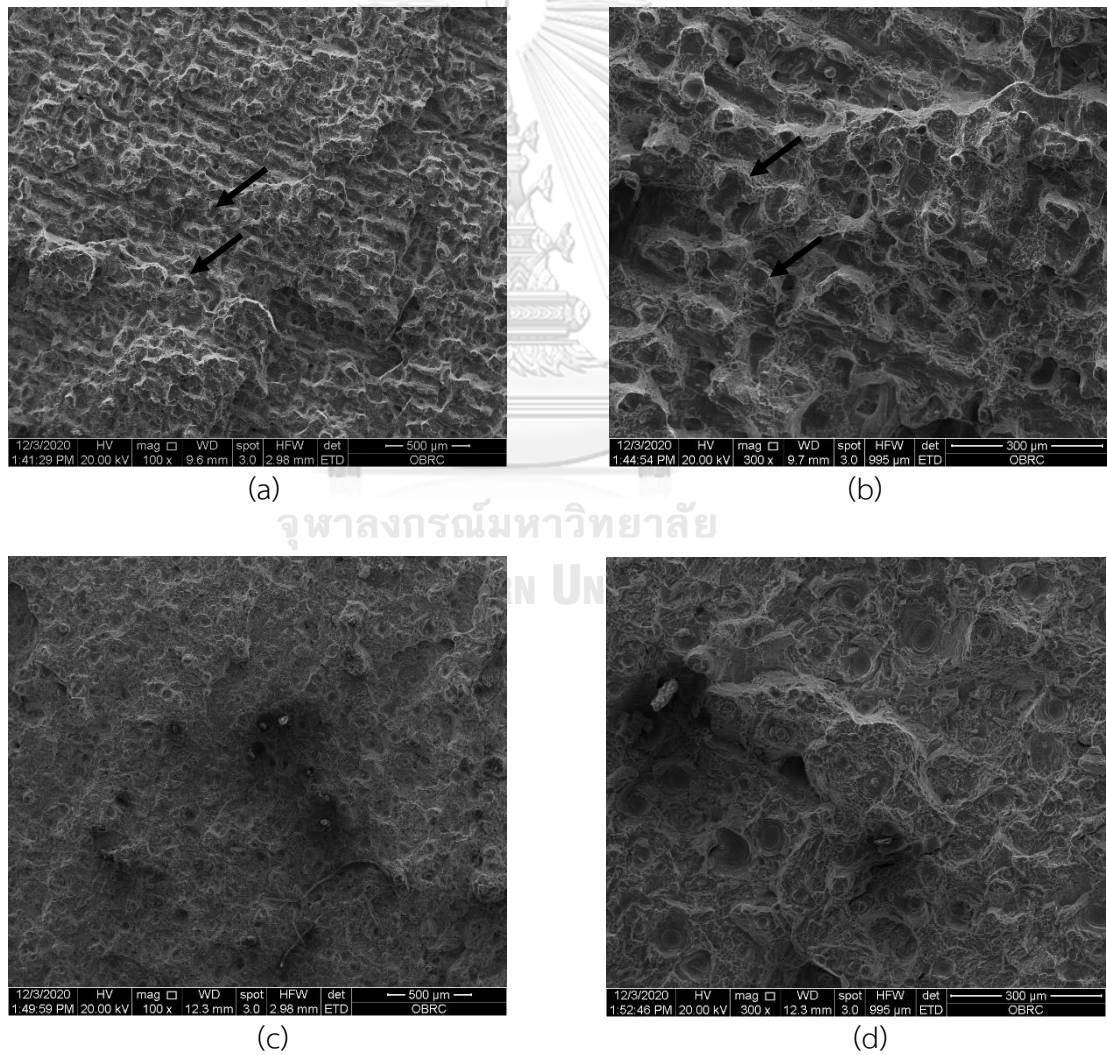
Figure 12 Fractographic images of 3 different SLM Ti-6Al-4V ELI groups. (a,b)75 W, (c,d)100 W and (e,f)125 W at x100 and x300 magnification, respectively. The dark arrows indicate the presence of the dimple fracture. The white arrows indicate the presence of the transgranular clevage facet.

The fractographic images from SEM at x100 and x300 magnification, In the group laser power 75 W (figure 12a and b) and 100 W (figure 12c and d) showed the characteristic in both ductile and brittle failure mode. But in the group laser power 75 W dominantly presented the ductile failure mode compared to the group laser power 100 W which was rounded outline fracture or dimple characteristic or honeycomb like characteristic. While in group laser power 125 W (figure 12e and f) showed the sharp border or transgranular cleavage facet which was the brittle failure mode.

Chapter V Discussion and conclusions

This study was perform to examine the differences in mechanical and physical properties of SLM Ti-6Al-4V ELI between different laser power. The first null hypothesis was rejected since the group of laser power 100 W showed a significantly higher mean tensile strength and microhardness compared to the other 2 groups.

The result of lower mean tensile strength and microhardness in the group laser power 75 and 125 can be explained by the microstructure. From optical microscope, we found some porosity in group of laser power 75 and 125 W (Figure 11a and 11c) dispersing through the specimen. The porosity resulted in the decreased tensile strength (42). We assumed that the lower laser power (low laser energy density) in the 75 W group could lead in less energy transferred to the melting pool and the decreased temperature during the SLM process. So it was resulted in lack of fusion and generated the pores or known as the balling effect (43). This effect caused the defected sample and irregularities (42, 44). On the contrary, the over-concentrated laser energy in group laser power 125 W will bring overburning which may influence the density of samples (25) leading to low tensile strength too. However, as previously stated the laser energy density does not depend on only laser power, the other parameters such as scan speed, layer thickness, scan spacing and scan strategy can affect the microstructure and mechanical properties too.

Moreover, the nearly fully density or less porosity (Figure 11b) or high density in the group laser power 100 W which were caused from the proper energy density could produce the good mechanical properties. That was contributed to the better energy transferring, gained the depths of heat penetration and enhanced wettability of the melting pool effected in good melting pool quality (19, 20, 44). So the samples from this group could improve both tensile strength and microhardness too.

In addition, the group of laser power 100 W was the only one group that conformed to the ASTM F136-13 (Standard specification for wrought Titanium-6Aluminium-4Vanadium ELI alloy for surgical implant application) that required the ultimate tensile strength above 860 MPa.

Furthermore, we could find the α' martensitic microstructure in the group laser power 100 W more than 2 others group as indicated by the dark arrow in Figure 11b. This phase was the main constituent phase in Ti-6Al-4V ELI which fabricated by SLM (45). Meanwhile, in conventional manufacturing method such as casting, wrought or in the improper processing parameter in SLM do not presence this phase (46). The α' martensitic microstructure was considerable strengthening effect the material (27). So this phase could enhance the mechanical property in both ultimate tensile strength and microhardness(27). While the others 2 groups did not presence the α' martensitic phase. Therefore the second null hypothesis was rejected. Consequently, the laser power of 100 W with other constant parameters (spot size 30 μm, scanning speed 600 mm/s, layer thickness 30 μm) represents the appropriate level of properties.

This study conforms to a study by Choo et al in 2019. But they studied in stainless steel and claimed that varying the laser power from 200 to 380 W with constant a scan speed 300 mm/s resulted in a reduction in porosity from 0.88 to 0.13 percent (47). Additionally, there is another study by Attar et al in commercially pure titanium varied the laser power from 70 to 250 W, scan speed 20-180 mm/s. They found that a laser power of 165 W and a scan speed of 138 mm/s produced the highest titanium density. They also claimed that increasing the laser power above 180 W did not improve the density of titanium. And the porosity or the defect related to the processing parameters effected the microstructural structure resulted

in decreased mechanical properties.

SEM fractography revealed that the failure mode in groups of laser power 75 and 100 W was a mixed failure mode (Figures 12a, b, c and d). However, when compared to the group of laser power 100 W (Figures 12c and d), the group of laser power 75 W extinguished many dimples (Figures 12a and b). Dimples or honeycomb-like patterns are characteristic of ductile fracture. But in group of laser power 125 W mostly showed the characteristic of brittle fracture. That was transgranular clevage facet (Figures 12e and f). Additionally, the cracks of tensile failure began and expanded around the porosity or defect (48). We supposed that the low mechanical properties in group of laser power 125 W may caused from the alpha case. The alpha case was caused by the too high laser power or oxygen exposed. It was the oxygen-enriched surface alloy or weak point layers (49, 50). This layers had a detrimental effected in microcracks caused brittle fracture(49) in this study. Moreovers, this group also found the least α' martensitic phase because the high laser power leaded the less gap of cool down temperature. So the mechanical properties of this group were the least when compared to other groups.

In accordance with the study by Sun et al. in 2018, they found that the fracture surface of the SLM Ti-6Al-4V sample exhibited both brittle and ductile fracture in high laser energy density. But the low energy density of the laser resulted in unmelted metal powder, the fractography revealed more dimples of ductile failure (45).

Limitation

The limitation is our studies did not investigate the effect of the scan strategy or building orientation during the printing process(51).   Recently more research studies this effect to the physical and mechanical properties.

Suggested further studies

Further research could study the effect of post treatment of SLM Ti-6Al-4V ELI alloy on mechanical properties. Moreover, the biological studied in SLM Ti-6Al-4V ELI alloy could be investigated.

Conclusion

The difference in laser power effected the mechanical and physical properties. The laser power 100 W showed the highest tensile strength and highest microhardness compared to the other 2 groups. And this group was found the α′ martensitic phase structure.

Clinical implication

This study may provide the better knowledge about the effect of laser power to SLM Ti-6Al-4V ELI in mechanical properties and the microstructure. And this may lead to improve the mechanical properties in medical and dental implant in the future.

Declaration of conflicting interest

The authors declare that there is no conflict of interest.

REFERENCES

1.   Wysocki B, Maj P, Sitek R, Buhagiar J, Kurzydłowski KJ, Święszkowski W. Laser and Electron Beam Additive Manufacturing Methods of Fabricating Titanium Bone Implants. Applied Sciences. 2017;7:657.

2.   Frazier WE. Metal Additive Manufacturing: A Review. Journal of Materials Engineering and Performance. 2014;23(6):1917-28.

3.   Trevisan F, Calignano F, Aversa A, Marchese G, Lombardi M, Biamino S, et al. Additive manufacturing of titanium alloys in the biomedical field: processes, properties and applications. Journal of Applied Biomaterials & Functional Materials. 2017;16.

4.   Yadroitsev I, Bertrand P, Smurov I. Parametric analysis of the selective laser melting process. Applied Surface Science. 2007;253(19):8064-9.

5.   Gross BC, Erkal JL, Lockwood SY, Chen C, Spence DM. Evaluation of 3D printing and its potential impact on biotechnology and the chemical sciences. Anal Chem. 2014;86(7):3240-53.

6.   Song B, Dong S, Zhang B, Liao H, Coddet C. Effects of processing parameters on microstructure and mechanical property of selective laser melted Ti6Al4V. Materials & Design. 2012;35:120-5.

7.   Agapovichev AV, Kokareva VV, Smelov VG, Sotov AV. Selective laser melting of titanium alloy: investigation of mechanical properties and microstructure. IOP Conference Series: Materials Science and Engineering. 2016;156:012031.

8.   Ahmad I, Al-Harbi F. 3D Printing in Dentistry - 2019/20202018.

9.   Azarniya A, Colera XG, Mirzaali MJ, Sovizi S, Bartolomeu F, St Weglowski Mk, et al. Additive manufacturing of Ti–6Al–4V parts through laser metal deposition (LMD): Process, microstructure, and mechanical properties. Journal of Alloys and Compounds. 2019;804:163-91.

10.   Sing SL, An J, Yeong WY, Wiria F. Laser and electron-beam powder-bed additive manufacturing of metallic implants: A review on processes, materials and designs. Journal of orthopaedic research : official publication of the Orthopaedic Research Society. 2015;34.

11.   Bisht M, Ray N, Verbist F, Coeck S. Correlation of selective laser melting-melt pool events with the tensile properties of Ti-6Al-4V ELI processed by laser powder bed fusion. Additive Manufacturing. 2018;22:302-6.

12.   Zhang L-C, Attar H. Selective Laser Melting of Titanium Alloys and Titanium Matrix Composites for Biomedical Applications: A Review Advanced Engineering Materials. 2016;18(4):463-75.

13.   Vilaro T, Colin C, Bartout JD. As-Fabricated and Heat-Treated Microstructures of the Ti-6Al-4V Alloy Processed by Selective Laser Melting. Metallurgical and Materials Transactions A. 2011;42(10):3190-9.

14.   Dutta B, Froes FH. The Additive Manufacturing (AM) of titanium alloys. Metal Powder Report. 2017;72(2):96-106.

15.   Vrancken B, Thijs L, Kruth J-P, Humbeeck J. Heat treatment of Ti6Al4V produced by Selective Laser Melting: Microstructure and Mechanical properties. Journal of Alloys and Compounds. 2012;541:177-85.

16.   Sing SL. Selective Laser Melting of Novel Titanium-Tantalum Alloy as Orthopaedic Biomaterial. [electronic resource]. 1st ed. 2019. ed: Springer Singapore; 2019.

17.   El-Sayed M, Ghazy M, Youssef YM, Essa K. Optimization of SLM process parameters for Ti6Al4V medical implants. Rapid Prototyping Journal. 2018.

18.   Wang Z, Li P. Characterisation and constitutive model of tensile properties of selective laser melted Ti-6Al-4V struts for microlattice structures. Materials Science and Engineering: A. 2018;725:350-8.

19.   Kusuma C, Ahmed SH, Mian A, Srinivasan R. Effect of Laser Power and Scan Speed on Melt Pool Characteristics of Commercially Pure Titanium (CP-Ti). Journal of Materials Engineering and Performance. 2017;26(7):3560-8.

20.   Elsayed M. Optimization of SLM process parameters for Ti6Al4V medical implants. Rapid Prototyping Journal. 2019;25(3):433-47.

21.   Liu J, Song Y, Chen C, Wang X, Li H, Zhou Ca, et al. Effect of scanning speed on the microstructure and mechanical behavior of 316L stainless steel fabricated by selective laser melting. Materials and Design. 2019:108355.

22.   Azarniya A, Garmendia X, Mirzaali MJ, Sovizi S, Bartolomeu F, Mare W, et al. Additive manufacturing of Ti–6Al–4V parts through laser metal deposition (LMD): Process, microstructure, and mechanical properties. Journal of Alloys and Compounds. 2019;804.

23.   Spierings A, Dawson K, Uggowitzer P, Wegener K. Influence of SLM scan-speed on microstructure, precipitation of Al 3 Sc particles and mechanical properties in Sc- and Zr-modified Al-Mg alloys. Materials & Design. 2017;140.

24.   Zhang B, Liao H, Coddet C. Effects of processing parameters on properties of selective laser melting Mg–9%Al powder mixture. Materials & Design. 2012;34:753-8.

25.   Sun J, Yang Y, Wang D. Parametric optimization of selective laser melting for forming Ti6Al4V samples by Taguchi method. Optics & Laser Technology. 2013;49:118-24.

26.   Phaiboonworachat A, Kourousis K. Cyclic Elastoplastic Behaviour, Hardness and Microstructural Properties of Ti-6Al-4V Manufactured through Selective Laser Melting. International Journal of Materials Engineering Innovation. 2016;7:80-7.

27.   Galarraga H, Warren RJ, Lados DA, Dehoff RR, Kirka MM, Nandwana P. Effects of heat treatments on microstructure and properties of Ti-6Al-4V ELI alloy fabricated by electron beam melting (EBM). Materials Science and Engineering: A. 2017;685:417-28.

28.   Qian M, Xu W, Brandt M, Tang HP. Additive manufacturing and postprocessing of Ti-6Al-4V for superior mechanical properties. MRS Bulletin. 2016;41(10):775-84.

29.   Levine BR, Sporer S, Poggie RA, Della Valle CJ, Jacobs JJ. Experimental and clinical performance of porous tantalum in orthopedic surgery. Biomaterials. 2006;27(27):4671-81.

30.   Murr LE, Quinones SA, Gaytan SM, Lopez MI, Rodela A, Martinez EY, et al. Microstructure and mechanical behavior of Ti–6Al–4V produced by rapid-layer manufacturing, for biomedical applications. Journal of the Mechanical Behavior of Biomedical Materials. 2009;2(1):20-32.

31.   Schulze C, Weinmann M, Schweigel C, Kessler O, Bader R. Mechanical Properties of a Newly Additive Manufactured Implant Material Based on Ti-42Nb. Materials (Basel). 2018;11(1).

32.   Vandenbroucke B, Kruth J-P. Selective laser melting of biocompatible metals for rapid manufacturing of medical parts. Rapid Prototyping Journal. 2007;13:196-203.

33.   Rengier F, Mehndiratta A, von Tengg-Kobligk H, Zechmann CM, Unterhinninghofen R, Kauczor HU, et al. 3D printing based on imaging data: review of medical applications. Int J Comput Assist Radiol Surg. 2010;5(4):335-41.

34.   Gross BC, Erkal JL, Lockwood SY, Chen C, Spence DM. Evaluation of 3D Printing and Its Potential Impact on Biotechnology and the Chemical Sciences. Analytical Chemistry. 2014;86(7):3240-53.

35.   Brunette DM, P. Tengvall, Textor M. Titanium in medicine: Springer; 2001.

36.   Yan Q, Dong H, Su J, Han J, Song B, Wei Q, et al. A Review of 3D Printing Technology for Medical Applications. Engineering. 2018;4(5):729-42.

37.   Han M-K, Kim J-Y, Hwang MJ, Song H-J, Park Y-J. Effect of Nb on the Microstructure, Mechanical Properties, Corrosion Behavior, and Cytotoxicity of Ti-Nb Alloys. Materials. 2015;8:5986-6003.

38.   Liu S, Shin YC. Additive manufacturing of Ti6Al4V alloy: A review. Materials & Design. 2019;164:107552.

39.   Gerd Lutjering, Williams JC. Titanium. second ed: Springer.

40.   Shunmugavel M, Polishetty A, Goldberg M, Singh R, Littlefair G. A comparative study of mechanical properties and machinability of wrought and additive manufactured (selective laser melting) titanium alloy-Ti-6Al-4V. Rapid Prototyping Journal. 2017;23:00-.

41.   ASTM. ASTM E8-04, Standard Test Methods for Tension Testing of Metallic Materials. 2004.

42.   Attar H, Calin M, Zhang LC, Scudino S, Eckert J. Manufacture by selective laser melting and mechanical behavior of commercially pure titanium. Materials Science and Engineering: A. 2014;593:170-7.

43.   Gu D, Hagedorn Y-C, Meiners W, Meng G, Batista RJS, Wissenbach K, et al. Densification behavior, microstructure evolution, and wear performance of selective laser melting processed commercially pure titanium. Acta Materialia. 2012;60(9):3849-60.

44.   Khorasani A, Gibson I, Awan US, Ghaderi A. The effect of SLM process parameters on density, hardness, tensile strength and surface quality of Ti-6Al-4V. Additive Manufacturing. 2019;25:176-86.

45.   Sun D, Gu D, Lin K, Ma J, Chen W, Huang J, et al. Selective laser melting of titanium parts: Influence of laser process parameters on macro- and microstructures and tensile property. Powder Technology. 2019;342:371-9.

46.   Shipley H, McDonnell D, Culleton M, Coull R, Lupoi R, O'Donnell G, et al. Optimisation of process parameters to address fundamental challenges during selective laser melting of Ti-6Al-4V: A review. International Journal of Machine Tools and Manufacture. 2018;128:1-20.

47.   Choo H, Sham K-L, Bohling J, Ngo A, Xiao X, Ren Y, et al. Effect of laser power on defect, texture, and microstructure of a laser powder bed fusion processed 316L stainless steel. Materials & Design. 2019;164:107534.

48.   Gong H, editor Generation and detection of defects in metallic parts fabricated by selective laser melting and electron beam melting and their effects on mechanical properties2013.

49.   Sefer B. Oxidation and Alpha–Case Phenomena in Titanium Alloys used in Aerospace Industry: Ti–6Al–2Sn–4Zr–2Mo and Ti–6Al–4V 2014.

50.   Gaddam R, Sefer B, Pederson R, Antti ML. Study of alpha-case depth in Ti-6Al-2Sn-4Zr-2Mo and Ti-6Al-4V. IOP Conference Series: Materials Science and Engineering. 2013;48:012002.

51.   Sing SL. Selective Laser Melting of Novel Titanium-Tantalum Alloy as Orthopaedic Biomaterial2019.

VITA

NAME   Pajaree Termrungruanglert

DATE OF BIRTH   9 January 1990

PLACE OF BIRTH   Bangkok, Thailand

INSTITUTIONS ATTENDED   Doctor of Surgery, Thammasat university